

RESEARCH PAPER

Silver-nanoparticle Supported on Nanocrystalline Cellulose using Cetyltrimethylammonium Bromide: Synthesis and Catalytic Performance for Decolorization of Dyes

Hannaneh Heidari*, Melika Karbalaee

Department of Chemistry, Faculty of Physics and Chemistry, Alzahra University, Tehran, Iran

ARTICLE INFO

Article History:

Received 16 September 2020

Accepted 28 December 2020

Published 01 January 2021

Keywords:

Cetyltrimethylammonium bromide

Dye

Nanocomposite

Nanocrystalline cellulose

Silver nanoparticles

ABSTRACT

In this work, we reported that the ultrasonically synthesized nanocrystalline cellulose (NCC) from microcrystalline cellulose has the capacity for use as natural and green matrices for the synthesis of silver nanoparticles. Cationic surfactant cetyltrimethylammonium bromide (CTAB) was employed as a modifier and stabilizer for NCC. The structure of as-synthesized composite (Ag/CTAB/NCC) was characterized by Fourier transform infrared spectroscopy (FT-IR); field emission scanning electron microscopy (FE-SEM); Transmission electron microscopy (TEM); Energy dispersive spectroscopy (EDS), and X-ray diffraction (XRD). The XRD pattern confirmed the single cubic phase of Ag nanoparticles with crystallite size about 30 nm. TEM study also verified that the average particle size of the spherical-shaped Ag NPs. catalytic activity of Ag/CTAB/NCC has been analyzed by performing the reduction of certain toxic azo methyl orange dye (MO) (by two methods) and aromatic nitro compound of 4-nitrophenol (4-NP) in shorter time. The reduction of MO to hydrazine derivatives and 4-NP to 4-aminophenol takes place with a pseudo-first-order rate constants. The reduction time regularly decreased and the rate of reduction (k) increases (3 fold) with increasing catalyst amount in method (2) (mmol NaBH₄/mmol MO = 250 and 42 mg catalyst) compared to method (1) (mmol NaBH₄/mmol MO = 400 and 5 mg catalyst). The results indicated that spherical AgNPs immobilized CTAB-adsorbed NCC showed better catalytic activity and shorter reduction time towards the removal of methyl orange ($k = 14.2 \times 10^{-3} \text{ s}^{-1}$, $t = 150 \text{ s}$) and 4-nitrophenol ($k = 5.4 \times 10^{-3} \text{ s}^{-1}$, $t = 180 \text{ s}$) compared with previous works that could be introduced as an effective method for the catalytic treatment of wastewater.

How to cite this article

Heidari H., Karbalaee M. Silver-nanoparticle Supported on Nanocrystalline Cellulose using Cetyltrimethylammonium Bromide: Synthesis and Catalytic Performance for Decolorization of Dyes. J Nanostruct, 2021; 11(1): 48-56. DOI: 10.22052/JNS.2021.01.006

INTRODUCTION

Over the last decade, nanostructured particles, especially inorganic nanoparticles (NPs), have received more attention in biomedical applications, materials science, and engineering [1-6].

Inorganic NPs, show special properties including tunable physicochemical characteristics,

high surface area to volume ratio, small size, increased numbers of atoms at the edges, and the corners which are surrounded by fewer atoms and considered to be more reactive [7, 8]. Among the inorganic NPs, silver as the most frequently used noble metal NPs has attracted considerable attention because of efficiency, cost

* Corresponding Author Email: h.heidari@alzahra.ac.ir

viability and the potential in various applications such as catalysis and antimicrobials [2, 3, 9, 10]. However, metal NPs tend to aggregate that minimizes their surface area and reduce their catalytic performance. One of the potential methods to overcome this problem is using hybrid inorganic-polymer nanocomposites. In this regard, environmentally benign natural polymers, like chitin, alginic acid, chitosan, and cellulose [11-14] related to hydrophilicity and multiple functionalities, having the strong ability to chelate metal ions could serve the purpose better.

NCC, as one of the natural biopolymers could be obtained from different sources such as cotton by using acid hydrolysis process as a common method [15]. However, other modified techniques including mechanical processes compared to acid hydrolysis have been developed which are simple, low cost, and environmentally friendly [16].

Generally, the deposition of metal NPs on the surface of NCC can be readily achieved using a strong reducing agent like NaBH_4 . Recently, various methods were applied for surface functionalization of NCC by chemical bonding to control morphology and particle size of metal nanoparticles using a surfactant [17]. Moreover, surfactant similar to other dispersants was utilized to prevent aggregation of NPs in the chemical reduction process [18].

Cetyltrimethylammonium bromide (CTAB), a cationic surfactant with multifunctional groups (alkyl chain and quaternary ammonium group as hydrophobic tail and hydrophilic head) with the abilities of reduction and/or coordination, has been used to stabilize inorganic NPs [18- 20].

Zaid et al. synthesized functionalized iron oxide with mercaptopropionic acid ($\text{MPA-Fe}_3\text{O}_4$) nanoparticle and commercial nanocellulose crystalline functionalized cetyl trimethyl ammonium bromide (NCC/CTAB) for DNA electrochemical biosensor. [21].

Manan et al. prepared commercial nanocrystalline cellulose (NCC) with cationic surfactant of cetyltrimethyl ammonium bromide (CTAB) and further decorated with 3-mercaptopropionic acid (3-MPA) capped CdS QDs as biosensor for phenol determination [22]. An et al. reported NCC/CTAB/Ag nanocomposite as a catalyst for the reduction of 4-Nitrophenol. Yalcinkaya et al. have synthesized NCC/CTAB/Ag nanocomposites for use in PLA films. NCC in all the above composites are prepared commercially or they are obtained by

sulphuric acid hydrolysis [7, 19]. However, in our study, NCC was prepared from microcrystalline cellulose by a simple and facile mechanical method using ultrasonication without acid hydrolysis as a common chemical process. It was used as green support/carrier for silver nanoparticle by CTAB as stabilizer.

Organic dyes were widely used and released by many industries, which have been attracting serious public concern due to environmental contamination [23, 24]. The anionic dye of methyl orange due to intense color, toxicity, and carcinogenic effects is a pollutant compound when released into the environment. 4-Nitrophenol is another toxic and chemically hazardous compound due to solubility and stability in the ordinary and wastewater systems. Numerous methods were used for the degradation of MO and 4-NP. Catalytic degradation of MO to hydrazine derivatives and 4-NP to 4-Aminophenol (4-AP) by metal nanoparticles is an important way without the production of secondary toxic substances [25-30]. Hence, developing an effective method for the degradation of these dyes from the environment is still a challenge. Recently, we reported the synthesis of Ag/NCC and its catalytic application in degradation of toxic dyes [16]. Here, NCC can be improved by using the surfactant for the synthesis of NCC/CTAB/Ag nanocomposite. The formation of cellulose base nanocomposite was confirmed by FTIR, FESEM, EDS, TEM and XRD characterization. This research reported an effective catalyst for highly efficient reduction of organic pollutants (MO and 4-NP) from environmental water within few minutes.

MATERIALS AND METHODS

All chemicals were purchased from Merck and Acros chemical Companies and were used without further purification. IR spectra were recorded from KBr disk using FT-IR Bruker Tensor 27 instrument. Fieldemission scanning electron microscopy (FE-SEM) with a FEI-Nanosem 450. Transmission electron microscopy (TEM) images have been taken with a Philips, model EM 208s. The energy dispersive spectroscopy (EDS) analysis was done using a SAMx-analyzer. The X-ray diffraction patterns (XRD) were obtained using a Phillips PW1730 X-ray diffractometer. The diffraction patterns were recorded using $\text{Cu-K}\alpha$ radiation at 40 kV and 30 mA. The samples were scanned in a 2θ range between 10 and 80. Ultraviolet-visible

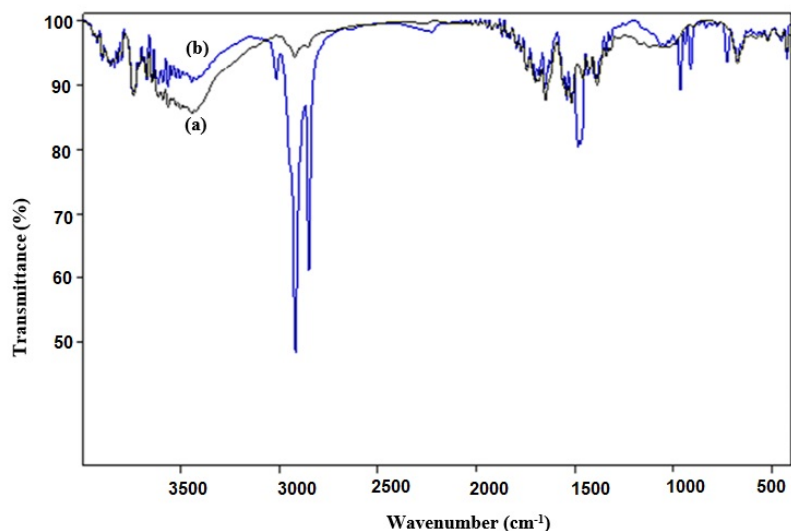


Fig. 1. FT-IR spectra of a) NCC b) Ag/CTAB/NCC

(UV-Vis) measurements were performed using Lambda-25 UV-Vis spectrometer.

Preparation of NCC

The mixture of microcrystalline cellulose in water (3 wt.%) put into ice/water bath and set in the ultrasonicator for 15 min at an output power of 1200 W. The obtained colloidal suspension was centrifuged, the supernatant was dried and stored at 5 °C [16].

Preparation of Ag /CTAB/ NCC nanocomposite

Synthesis of Ag nanocomposite was carried out in a typical experiment with some modification, [9] in which NCC suspension was diluted into 0.2 wt.% followed by sonification for 10 min. Then, in the 100 mL beaker in pH ~ 4.5, CTAB solution (30 mL, 0.5 mM) was added into the NCC suspension followed by the addition of a dropwise silver nitrate solution (20 mL, 0.1 mM). After that, aqueous sodium borohydride solution (20 mL, 10 mM) was added dropwise into the well-mixed suspension under constant magnetic stirring for 5 min the solution was then washed with distilled water and dried in an oven at 60 °C.

Catalytic removal of dye

Method 1:

The catalytic reduction of methyl orange was carried out in UV cuvette using methyl orange (0.05 mM, 2.5 mL), and sodium borohydride solution (0.1 M, 0.5 mL) in presence of 5 mg of the

dried composite as a catalyst. The color change of the solution was observed and the absorbance of resulting solutions was monitored using UV-Vis spectrophotometer.

Method 2:

An aqueous suspension of 42 mg of the dried composite was added into a mixed aqueous solution containing methyl orange or 4-nitrophenol (0.25 ml, 20 mM), sodium borohydride solution (0.25 ml, 5M), and 19.5 ml DI water under stirring at room temperature. Then, an aliquot of the reaction mixture (0.5 mL) at the appropriate intervals was filtered, the absorbance of the filtrate was recorded using a UV-Vis spectrophotometer in the wavelength range of 250-550 nm. The reaction rate was measured as a function of time [31].

RESULTS AND DISCUSSION

Characterization of catalyst

In the present work, NCC prepared from MCC, NCC analysis and the difference with MCC were discussed in our previous work [16]. Here we describe the characterization of the as-prepared composite.

The FTIR spectra of NCC and Ag /CTAB/ NCC composite are shown in (Fig. 1). NCC showed broad band at 3450 cm⁻¹, which can be assigned to the stretching vibration of hydroxyl groups. The peaks at 2850 and 2900 cm⁻¹ were related to the stretching of C-H. The bands at 1645, 1420, and 1010 cm⁻¹ were attributed to water absorption, -CH₂ groups, and the C-O-C stretching, respectively.

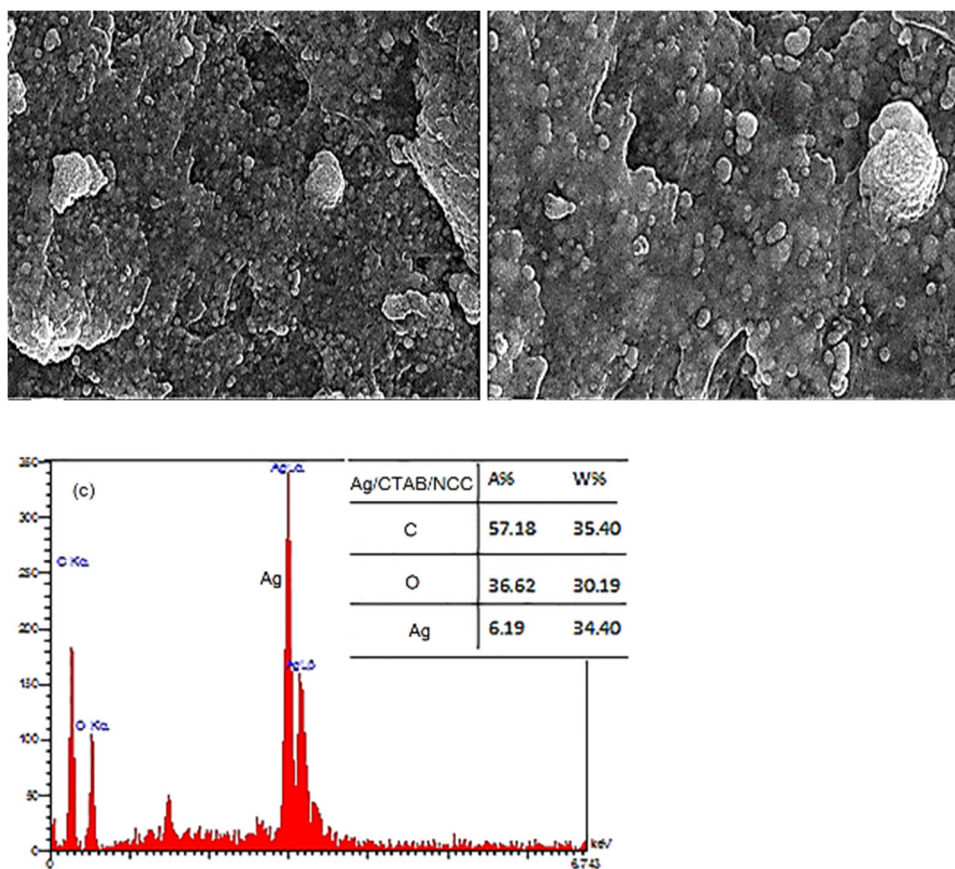


Fig. 2. FE-SEM images of a, b) Ag/CTAB/NCC and c) EDS spectrum of Ag/CTAB/NCC

For the Ag /CTAB/ NCC composite, a decreased intensity of the bands at 3450 cm^{-1} and 1010 cm^{-1} corresponding to the O-H and C-O stretching confirms the grafting of AgNPs to the O-H groups on the NCC surfaces was effective [7].

Fig. 2a, b showed the FE-SEM image of the Ag /CTAB/ NCC nanocomposite. In SEM images, a large number of spherical NPs were distributed on the surface of nanocellulose indicating that the formation of Ag nanoparticles. The EDS spectrum of nanocomposite is presented in (Fig. 2c). It exhibits the presence of C, O, and Ag elements. The intense peak at around 3 keV related to the Ag signal. Indicating the Ag had been successfully loaded on the surface of nanocellulose.

The TEM images of Ag/ CTAB/NCC nanocomposite with different magnification revealed the formation of spherical Ag nanoparticles with an average size between 20 and 50 nm and good dispersity on the surface of NCC. The images showed the loading of small particle size of spherical AgNPs with high dispersity

and low aggregation that can be attributed to the binding of Ag nanoparticles to the ammonium ions of the CTAB as a surfactant [19].

The crystalline structure of the as-prepared product was determined using XRD (Fig. 4). X-ray diffractogram of Ag/ CTAB/NCC was attributed to the characteristic peaks at 38.17° , 44.37° , 64.52° , 77.42° indexed as (111), (200), (220) and (311) crystallographic planes of the face-centered cubic (fcc) structure of Ag NPs on the NCC support (JCPDS 4-783) [32]. The sharp peaks of materials without reflections related to impurities phases show that the nanoparticles have the perfect phase purity and high crystallinity. Crystallite size of the silver nanoparticles was calculated about 30 nm through XRD analysis using Scherrer's formula (Eq. (1):

Where d is the average particle size, λ is X-ray wavelength (0.154 nm), β is FWHM of the diffraction line (radian), θ is the diffraction angle, and K constant, generally assumed as 0.9.

$$d = \frac{k\lambda}{\beta \cos \theta} \quad (1)$$

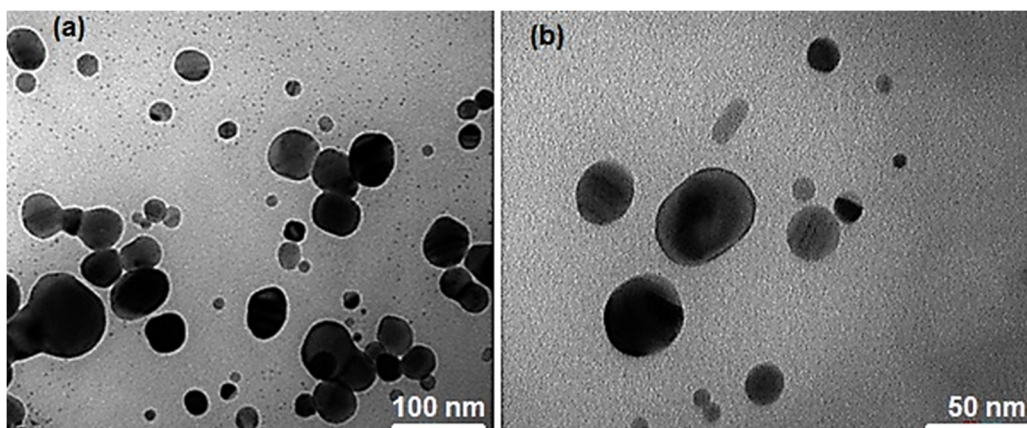


Fig. 3. TEM images at different magnifications (100 nm and 50 nm) of Ag/CTAB/NCC

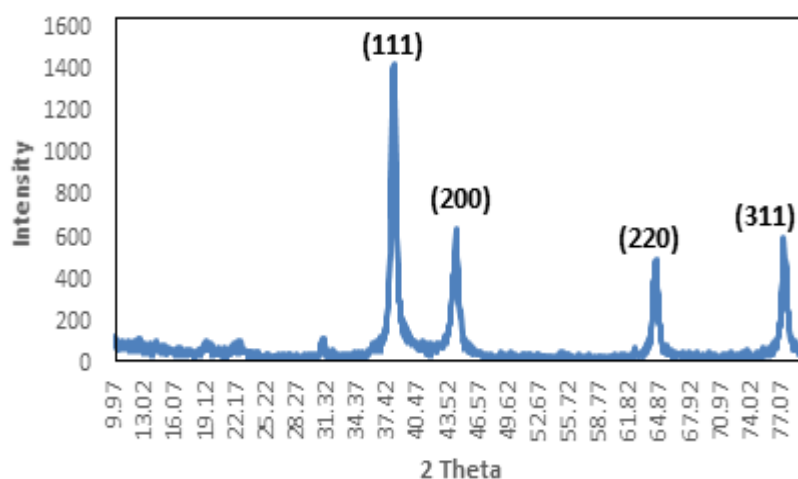


Fig. 4. XRD patterns of Ag/CTAB/NCC composite

Catalytic activity

To investigate the catalytic performance of the Ag/CTAB/NCC nanocatalyst in the presence of NaBH_4 , methyl orange dye was used. Fig. 5a, b show a typical evolution of the UV-Vis spectra of methyl orange during catalytic reduction after the addition of NaBH_4 via method (1) and 2, respectively. It is well known that the spectrum of methyl orange shows a peak at 465 nm [33]. After the addition of newly synthesized nanocomposite, the spectral band of MO is disappeared at 465 nm after 180 s in method 1 (Fig. 5a) and 150 s in method 2 (Fig. 5b). A new band appears at 250 nm which is assigned to hydrazine derivatives by changing the color from orange to colorless [33]. When the nanocatalyst was added for the reduction of 4-NP, the peak of 4-nitrophenolate ion (~ 400 nm) faded gradually. Meanwhile, a new

absorption peak at 298 nm increased intensity with reaction time. The appearance of such peak was taken as evidence for the formation of 4-AP [34]. The catalytic degradation at ambient conditions was complete within 180 s (Fig. 5c).

The linear plots of $\ln(A_t/A_0)$ versus reduction time for the MO catalytic reduction over the Ag/CTAB/NCC composite were shown in Fig. 6. Reaction rates are determined by measuring the absorbance values at 465 nm as a function of time. Generally, the reduction reaction can be assumed as pseudo-first-order kinetics due to excess concentration of NaBH_4 compared to MO dye. It can be described by the Langmuir-Hinshelwood equation [35]. The rate constant of the catalyst was estimated directly by the slope of the linear graph $4.8 \times 10^{-3} \text{ s}^{-1}$ by method 1 (Fig. 6a). and $14.2 \times 10^{-3} \text{ s}^{-1}$ by method 2 (Fig. 6b) for MO and 5.4×10^{-3}

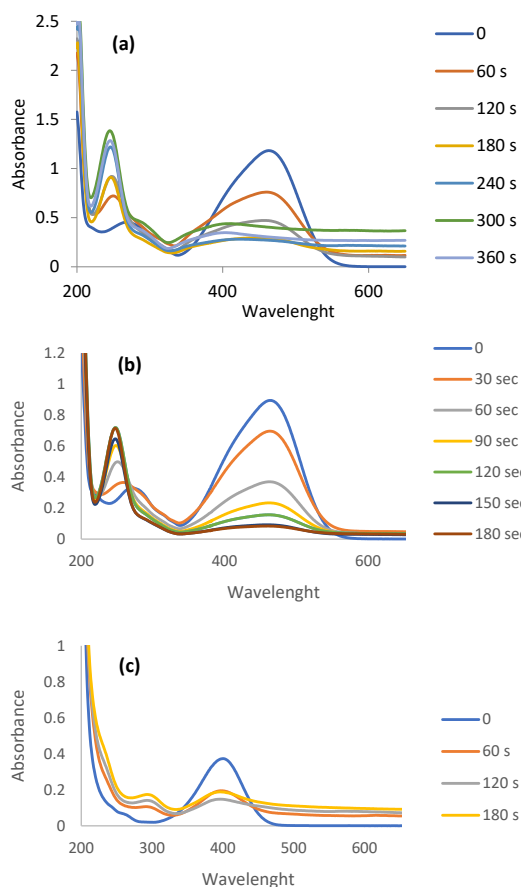


Fig. 5. UV-Vis spectra of MO aqueous solution a) method 1), b) method (2), c) UV-Vis spectra of 4-NP aqueous solution with method 2

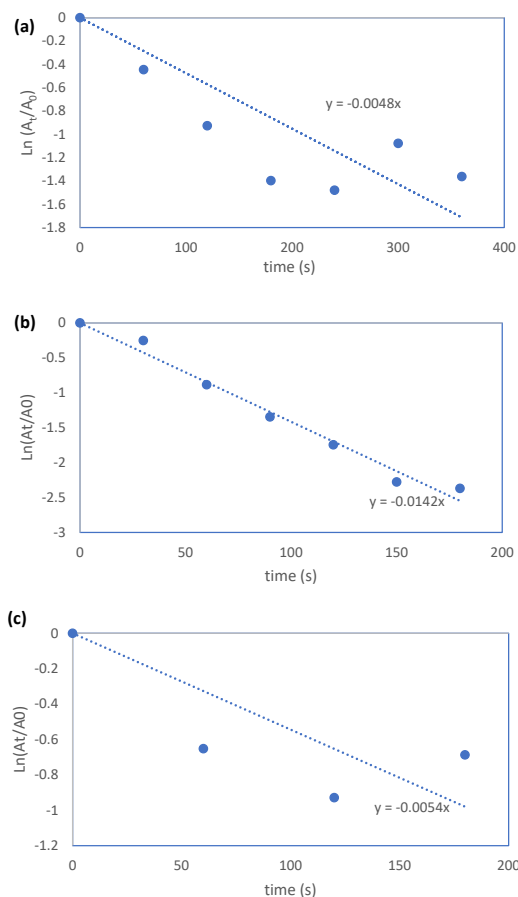


Fig. 6. The plot of $\ln A_t/A_0$ versus time for the reduction of MO using a) method (1), b) mehod (2), and c) The plot of $\ln A_t/A_0$ versus time for the reduction of 4-NP using method (1)

Table 1. Comparison of this work results with other catalysts reported in the reduction of MO

Entry	Catalyst	$k \times 10^{-3} (s^{-1})$	Ref
1	Ag@NCC	12.3	[16]
2	Ag NPs	0.09	[8]
3	Pd ₇₅ Au ₃₅ /Dens-OH	5.87	[36]
4	AgNP-DT	5.34	[37]
5	Ag/ CTAB/NCC	14.2	This work

s^{-1} for 4-NP (Fig. 6c).

To compare the catalytic activity of the nanocomposite with the other reported catalysts including Ag NPs used for the reduction of MO and 4-NP, the rate constants, k , were summarized

in Table 1 and Table 2, respectively. The catalytic activity of this catalyst is comparable with other listed catalysts in Tables 1 and 2. As shown in Table 2, the differences between the reaction rate constants of NCC/CTAB/ Ag (Ref. [19]) (1.6

Table 2. Comparison of this work results with other catalysts reported in the reduction of 4-NP

Entry	Catalyst	$k \times 10^{-3} (s^{-1})$	Ref
1	NCC/CTAB/ Ag	1.6	[19]
2	T-ZnO-rGO-PEI	3.7	[38]
3	PP-g-EDA@Ag/Cu	4.1	[39]
4	CS-CNTs-PdNPs	3.6	[40]
5	Ag/ CTAB/NCC	5.4	This work

$\times 10^{-3} s^{-1}$) and Ag/ CTAB/NCC in this work ($5.4 \times 10^{-3} s^{-1}$), are as follows: addition to difference in NCC preparation method as support, the concentration of 4-NP and reducing agent ($NaBH_4$) also the amount of catalyst are different. In ref [19], the molar ratio of sodium borohydride to 4-nitrophenol (mmol $NaBH_4$ / mmol 4-Np) is 100 and the aqueous suspension of CNC/ CTAB/ Ag nanocatalyst contains 0.02 μ mol Ag. While in this work, the molar ratio (mmol $NaBH_4$ / mmol 4-Np) increased to 250 and 42 mg of composite was used. Due to the aforementioned differences, the reaction rate constant in this work is almost 3 times higher than that mentioned in ref [19].

CONCLUSION

The nanohybrid (Ag/CTAB/NCC), consists of environmentally benign components Ag and NCC as support for Ag nanoparticles in which NCC was prepared using the sonication process without acid hydrolysis. Ag NPs was also stabilized on NCC surface using CTAB. The nanocomposite demonstrated high catalytic efficiency in reduction of MO and 4-NP by $NaBH_4$. The effect of the catalyst amount in enhancing the reduction rate was shown by comparing the reduction process in the two methods, which is about three times higher for that of employing higher amount of catalyst. Increasing of catalyst provides more active sites for binding of reducing agent and organic dye. The corresponding pseudo-first-order rate constants for reduction of MO increased with the method (2) ($14.2 \times 10^{-3} s^{-1}$) as compared to those exhibited by the method (1) ($4.8 \times 10^{-3} s^{-1}$). Besides, this catalyst reduced 4-NP to 4-AP via the method (2) by a rate constant of $5.4 \times 10^{-3} s^{-1}$. The results showed that Ag /CTAB/ NCC nanocatalyst has strong catalytic properties compared to other

reported catalysts. This green and cost-effective nanocatalyst expands the application of inorganic nano-metal composites for use in environmental protection.

ACKNOWLEDGEMENT

The authors gratefully acknowledge from the Research Council of Alzahra University for financial support.

CONFLICTS OF INTEREST

The authors declare that there are no conflicts of interest regarding the publication of this manuscript.

REFERENCES

- Otitoju TA, Ahmadipour M, Li S, Shoparwe NF, Jie LX, Owolabi AL. Influence of nanoparticle type on the performance of nanocomposite membranes for wastewater treatment. *Journal of Water Process Engineering*. 2020;36:101356.
- Ahmad MA, Salmiati S, Marpongahtun M, Salim MR, Lolo JA, Syaifuddin A. Green Synthesis of Silver Nanoparticles Using *Muntingia calabura* Leaf Extract and Evaluation of Antibacterial Activities. *Biointerface Res Appl Chem*. 2020;10:6253.
- Khan T, Yasmin A, Townley HE. An evaluation of the activity of biologically synthesized silver nanoparticles against bacteria, fungi and mammalian cell lines. *Colloids and Surfaces B: Biointerfaces*. 2020;194:111156.
- Kheiri S, Mohamed MGA, Amereh M, Roberts D, Kim K. Antibacterial efficiency assessment of polymer-nanoparticle composites using a high-throughput microfluidic platform. *Materials Science and Engineering: C*. 2020;111:110754.
- Chen X, Lin H, Xu T, Lai K, Han X, Lin M. Cellulose nanofibers coated with silver nanoparticles as a flexible nanocomposite for measurement of flusilazole residues in Oolong tea by surface-enhanced Raman spectroscopy. *Food Chemistry*. 2020;315:126276.
- Cho H-J, Kim I-D, Jung SM. Multifunctional Inorganic Nanomaterial Aerogel Assembled into fSWNT Hydrogel Platform for Ultrasensitive NO_2 Sensing. *ACS Applied*

- Materials & Interfaces. 2020;12(9):10637-47.
7. Yalcinkaya EE, Puglia D, Fortunati E, Bertoglio F, Bruni G, Visai L, et al. Cellulose nanocrystals as templates for cetyltrimethylammonium bromide mediated synthesis of Ag nanoparticles and their novel use in PLA films. *Carbohydrate Polymers*. 2017;157:1557-67.
 8. Islam MT, Saenz-Arana R, Wang H, Bernal R, Noveron JC. Green synthesis of gold, silver, platinum, and palladium nanoparticles reduced and stabilized by sodium rhodizonate and their catalytic reduction of 4-nitrophenol and methyl orange. *New Journal of Chemistry*. 2018;42(8):6472-8.
 9. Xiong R, Lu C, Wang Y, Zhou Z, Zhang X. Nanofibrillated cellulose as the support and reductant for the facile synthesis of Fe₃O₄/Ag nanocomposites with catalytic and antibacterial activity. *Journal of Materials Chemistry A*. 2013;1(47):14910.
 10. M. Kaloti, A. Kumar, Sustainable Catalytic Activity of Ag-Coated Chitosan-Capped γ -Fe₂O₃ Superparamagnetic Binary Nanohybrids (Ag- γ -Fe₂O₃@CS) for the Reduction of Environmentally Hazardous Dyes - A Kinetic Study of the Operating Mechanism Analyzing Methyl Orange Reduction, *ACS Omega*. 2018; 3:1529.
 11. Duan B, Liu F, He M, Zhang L. Ag-Fe₃O₄ nanocomposites@ chitin microspheres constructed by in situ one-pot synthesis for rapid hydrogenation catalysis. *Green Chem*. 2014;16(5):2835-45.
 12. Venkatesham M, Ayodhya D, Madhusudhan A, Veera Babu N, Veerabhadram G. A novel green one-step synthesis of silver nanoparticles using chitosan: catalytic activity and antimicrobial studies. *Applied Nanoscience*. 2012;4(1):113-9.
 13. Supriya, Kaspate R, Pal CK, Sengupta S, Basu JK. Microwave-mediated synthesis of silver nanoparticles on various metal-alginate composites: evaluation of catalytic activity and thermal stability of the composites in solvent-free acylation reaction of amine and alcohols. *SN Applied Sciences*. 2020;2(2).
 14. Kwiczak-Yigitbaşı J, Demir M, Ahan RE, Canlı S, Şafak Şeker UÖ, Baytekin B. Ultrasonication for Environmentally Friendly Preparation of Antimicrobial and Catalytically Active Nanocomposites of Cellulosic Textiles. *ACS Sustainable Chemistry & Engineering*. 2020;8(51):18879-88.
 15. Nandi S, Guha P. A Review on Preparation and Properties of Cellulose Nanocrystal-Incorporated Natural Biopolymer. *Journal of Packaging Technology and Research*. 2018;2(2):149-66.
 16. Heidari H, Karbalaee M. Ultrasonic assisted synthesis of nanocrystalline cellulose as support and reducing agent for Ag nanoparticles: green synthesis and novel effective nanocatalyst for degradation of organic dyes. *Applied Organometallic Chemistry*. 2019:e5070.
 17. Mariano M, El Kissi N, Dufresne A. Cellulose nanocrystals and related nanocomposites: Review of some properties and challenges. *Journal of Polymer Science Part B: Polymer Physics*. 2014;52(12):791-806.
 18. Li X, Shen J, Du A, Zhang Z, Gao G, Yang H, et al. Colloids and Surfaces A: Physicochemical and Engineering Aspects Facile synthesis of silver nanoparticles with high concentration via a CTAB-induced silver mirror reaction. 2012;400:73.
 19. An X, Long Y, Ni Y. Cellulose nanocrystal/hexadecyltrimethylammonium bromide/silver nanoparticle composite as a catalyst for reduction of 4-nitrophenol. *Carbohydrate Polymers*. 2017;156:253-8.
 20. Khan Z, Al-Thabaiti SA, Obaid AY, Khan ZA, Al-Youbi AAO. Shape-directing role of cetyltrimethylammonium bromide in the preparation of silver nanoparticles. *Journal of Colloid and Interface Science*. 2012;367(1):101-8.
 21. Mat Zaid MH, Che-Engku-Chik CEN, Yusof NA, Abdullah J, Othman SS, Issa R, et al. DNA Electrochemical Biosensor Based on Iron Oxide/Nanocellulose Crystalline Composite Modified Screen-Printed Carbon Electrode for Detection of Mycobacterium tuberculosis. *Molecules*. 2020;25(15):3373.
 22. Manan FAA, Hong WW, Abdullah J, Yusof NA, Ahmad I. Nanocrystalline cellulose decorated quantum dots based tyrosinase biosensor for phenol determination. *Materials Science and Engineering: C*. 2019;99:37-46.
 23. Li J, Zhang S, Chen Y, Liu T, Liu C, Zhang X, et al. A novel three-dimensional hierarchical CuAl layered double hydroxide with excellent catalytic activity for degradation of methyl orange. *RSC Advances*. 2017;7(46):29051-7.
 24. Bakhsh EM, Khan SA, Marwani HM, Danish EY, Asiri AM, Khan SB. Performance of cellulose acetate-ferric oxide nanocomposite supported metal catalysts toward the reduction of environmental pollutants. *International Journal of Biological Macromolecules*. 2018;107:668-77.
 25. Veksha A, Pandya P, Hill JM. The removal of methyl orange from aqueous solution by biochar and activated carbon under microwave irradiation and in the presence of hydrogen peroxide. *Journal of Environmental Chemical Engineering*. 2015;3(3):1452-8.
 26. Zhong W, Jiang T, Dang Y, He J, Chen S-Y, Kuo C-H, et al. Mechanism studies on methyl orange dye degradation by perovskite-type LaNiO₃- δ under dark ambient conditions. *Applied Catalysis A: General*. 2018;549:302-9.
 27. Saikia P, Miah AT, Das PP. Highly efficient catalytic reductive degradation of various organic dyes by Au/CeO₂-TiO₂ nano-hybrid. *Journal of Chemical Sciences*. 2017;129(1):81-93.
 28. Kurtan U, Amir M, Yıldız A, Baykal A. Synthesis of magnetically recyclable MnFe₂O₄@SiO₂@Ag nanocatalyst: Its high catalytic performances for azo dyes and nitro compounds reduction. *Applied Surface Science*. 2016;376:16-25.
 29. Kaloti M, Kumar A. Sustainable Catalytic Activity of Ag-Coated Chitosan-Capped γ -Fe₂O₃ Superparamagnetic Binary Nanohybrids (Ag- γ -Fe₂O₃@CS) for the Reduction of Environmentally Hazardous Dyes - A Kinetic Study of the Operating Mechanism Analyzing Methyl Orange Reduction. *ACS Omega*. 2018; 3:1529.
 30. Chiu H, Wi-afedzi T, Liu Y, Ghanbari F, Lin KA. *Journal of Water Process Engineering Cobalt Oxides with Various 3D Nanostructured Morphologies for Catalytic Reduction of 4-Nitrophenol : A Comparative Study*. *J Water Process Eng*. 2020;37:101379.
 31. Xiao S, Xu W, Ma H, Fang X. Size-tunable Ag nanoparticles immobilized in electrospun nanofibers: synthesis, characterization, and application for catalytic reduction of 4-nitrophenol. *RSC Adv*. 2012;2(1):319-27.
 32. Li Z, Jia Z, Ni T, Li S. Green and facile synthesis of fibrous Ag/cotton composites and their catalytic properties for 4-nitrophenol reduction. *Applied Surface Science*. 2017;426:160-8.
 33. Vidhu VK, Philip D. Catalytic degradation of organic dyes using biosynthesized silver nanoparticles. *Micron*.

- 2014;56:54-62.
34. Eisa WH, Abdelgawad AM, Rojas OJ. Solid-State Synthesis of Metal Nanoparticles Supported on Cellulose Nanocrystals and Their Catalytic Activity. *ACS Sustainable Chemistry & Engineering*. 2018;6(3):3974-83.
 35. Lu Y, Mei Y, Schrunner M, Ballauff M, Möller MW, Breu J. In Situ Formation of Ag Nanoparticles in Spherical Polyacrylic Acid Brushes by UV Irradiation. *The Journal of Physical Chemistry C*. 2007;111(21):7676-81.
 36. Dendrimer N. Effective Catalytic Reduction of Methyl Orange Catalyzed by the Encapsulated Random Alloy Palladium-Gold. *Chemistry Select* 2017;2:9803.
 37. Cyril N, George JB, Joseph L, Sylas VP. Catalytic Degradation of Methyl Orange and Selective Sensing of Mercury Ion in Aqueous Solutions Using Green Synthesized Silver Nanoparticles from the Seeds of *Derris trifoliata*. *Journal of Cluster Science*. 2019;30(2):459-68.
 38. Ramu AG, Yang DJ, Al Olayan EM, AlAmri OD, Aloufi AS, Almushawwah JO, et al. Synthesis of hierarchically structured T-ZnO-rGO-PEI composite and their catalytic removal of colour and colourless phenolic compounds. *Chemosphere*. 2021;267:129245.
 39. Zhang X-Q, Shen R-F, Guo X-J, Yan X, Chen Y, Hu J-T, et al. Bimetallic Ag-Cu nanoparticles anchored on polypropylene (PP) nonwoven fabrics: Superb catalytic efficiency and stability in 4-nitrophenol reduction. *Chemical Engineering Journal*. 2021;408:128018.
 40. Zhu J, Zhang X, Qin Z, Zhang L, Ye Y, Cao M, et al. Preparation of PdNPs doped chitosan-based composite hydrogels as highly efficient catalysts for reduction of 4-nitrophenol. *Colloids and Surfaces A: Physicochemical and Engineering Aspects*. 2021;611:125889.